Comparisons of classical chemical dynamics simulations of the unimolecular decomposition of classical and quantum microcanonical ensembles

Paranjothy Manikandan and William L. Hase

Citation: The Journal of Chemical Physics **136**, 184110 (2012); doi: 10.1063/1.4714219
View online: http://dx.doi.org/10.1063/1.4714219
View Table of Contents: http://scitation.aip.org/content/aip/journal/jcp/136/18?ver=pdfcov
Published by the AIP Publishing

Comparisons of classical chemical dynamics simulations of the unimolecular decomposition of classical and quantum microcanonical ensembles

Paranjothy Manikandan and William L. Hase
Department of Chemistry and Biochemistry, Texas Tech University, Lubbock, Texas 79409-1061, USA

(Received 7 March 2012; accepted 25 April 2012; published online 14 May 2012)

Previous studies have shown that classical trajectory simulations often give accurate results for short-time intramolecular and unimolecular dynamics, particularly for initial non-random energy distributions. To obtain such agreement between experiment and simulation, the appropriate distributions must be sampled to choose initial coordinates and momenta for the ensemble of trajectories. If a molecule's classical phase space is sampled randomly, its initial decomposition will give the classical anharmonic microcanonical (RRKM) unimolecular rate constant for its decomposition. For the work presented here, classical trajectory simulations of the unimolecular decomposition of quantum and classical microcanonical ensembles, at the same fixed total energy, are compared. In contrast to the classical microcanonical ensemble, the quantum microcanonical ensemble does not sample the phase space randomly. The simulations were performed for CH_4, C_2H_5, and Cl^----CH_3Br using both analytic potential energy surfaces and direct dynamics methods. Previous studies identified intrinsic RRKM dynamics for CH_4 and C_2H_5, but intrinsic non-RRKM dynamics for Cl^----CH_3Br. Rate constants calculated from trajectories obtained by the time propagation of the classical and quantum microcanonical ensembles are compared with the corresponding harmonic RRKM estimates to obtain anharmonic corrections to the RRKM rate constants. The relevance and accuracy of the classical trajectory simulation of the quantum microcanonical ensemble, for obtaining the quantum anharmonic RRKM rate constant, is discussed. © *2012 American Institute of Physics*. [http://dx.doi.org/10.1063/1.4714219]

I. INTRODUCTION

Classical trajectory simulations are widely used to study the intramolecular and unimolecular dynamics of highly vibrationally excited molecules.[1–8] Pathways and bottlenecks for intramolecular vibrational energy redistribution (IVR) may be investigated.[4,5,9] Of specific interest is identifying and understanding molecular properties which restrict the intramolecular flow of vibrational energy,[10–13] and initial rates of IVR may be compared with experiment.[14–16] A unimolecular rate constant determined from a simulation may be compared with the prediction of RRKM theory.[1,8]

A direct comparison with RRKM theory may be made by sampling the classical phase space randomly and simulating the unimolecular decomposition of a classical microcanonical ensemble of states.[1,2] The quantity of interest is the lifetime distribution $P(t)$, i.e.,

$$P(t) = -\frac{1}{N(0)}\frac{dN(t)}{dt}, \tag{1}$$

where $N(t)$ is the number of molecules, i.e., phase space points, remaining versus time. The $t = 0$ rate constant for this microcanonical ensemble is that of classical RRKM theory.[17] The assumption of RRKM theory is that as a result of rapid IVR this ensemble is maintained as the molecule decomposes, and at any time the molecule's unimolecular rate constant is that of classical RRKM theory. The molecule then decomposes exponentially with a rate constant given by classical RRKM theory and the lifetime distribution is

$$P(t) = ke^{-kt}. \tag{2}$$

Here $P(0) = k = k_{RRKM}$. This type of dynamics is referred to as *intrinsic* RRKM behavior.[3]

The contrasting dynamics is *intrinsic* non-RRKM behavior for which the unimolecular decay of the initial microcanonical ensemble is non-exponential.[3] The $t = 0$ rate constant will be that of classical RRKM theory, since there is a microcanonical ensemble at this time. However, the ensuing short time decomposition will have a rate constant longer than that of RRKM theory[18] and the rate constant for the long time decomposition will be smaller than that of RRKM theory. The complete non-exponential decomposition may be quite complex with multiple time scales,[19] i.e.,

$$\frac{N(t)}{N(0)} = \sum_i f_i e^{-k_i t}. \tag{3}$$

There is considerable interest in understanding classical phase space structures which lead to intrinsic non-RRKM dynamics.[9,18,20,21]

In comparing classical unimolecular rate constants with experimental and/or quantum values it is meaningful to separately consider molecules with intrinsic RRKM and non-RRKM dynamics. For intrinsic RRKM dynamics, an important consideration is that the chaotic classical dynamics does not conserve zero-point energy (ZPE). Thus, the barrier for the microcanonical ensemble of trajectories is the

classical barrier. In contrast, the quantum barrier, which includes ZPE, is much larger, and except for very high energies and/or small molecules the classical microcanonical unimolecular rate is larger than the quantum values.[22] For small molecules the ZPE is small and, if the classical dynamics is intrinsically RRKM, there is good agreement between the classical and quantum rate constants. Quantum state specific unimolecular resonance rate constants have been calculated for HO_2 (Ref. 23) and NO_2 (Ref. 24) dissociation, whose classical unimolecular dynamics is ergodic, and the classical RRKM rate constant is in good agreement with the average of these state specific rate constants for a small energy interval $E \rightarrow \Delta E$. For larger molecules with low barriers classical dynamics gives an accurate quantum microcanonical rate constant,[25,26] but if there is a substantial barrier the classical and quantum microcanonical rate constants only agree at high energies.[27]

If the classical dynamics is intrinsically non-RRKM, relationships between the classical and quantum dynamics are more complex and depend on the structure of the classical phase space.[22] A small molecule decomposes via isolated resonance states and for intrinsic non-RRKM dynamics, the molecule's phase space will consist of different types of trajectories including chaotic, quasiperiodic, and vague tori.[17,22] Resonance states corresponding to quasiperiodic trajectories are trapped in the molecule's phase space and will not dissociate.[28] In contrast, quantum mechanically the resonance state will "tunnel"[29] to products and have a finite lifetime. Trajectories may give accurate lifetimes for short-lived resonances, which correspond to classical chaotic motion as discussed above for HO_2 and NO_2. The correspondence between classical and quantum dynamics for classical motion intermediate between chaotic and quasiperiodic, e.g., vague tori, is less certain.[17]

The classical dynamics of the initial decomposition for a non-randomly excited molecule may be in accord with experiment. ZPE flow may be unimportant at these short times and the classical dynamics may recover the short-time vibrational adiabaticity. An illustration of this is the comparison of the classical dynamics of benzene C–H overtone states.[14–16] Classical dynamics describes the initial decay of the overtone state and, thus, gives an accurate linewidth for the overtone absorption transition.[15,16] An example of good agreement between classical and experimental rate constants for both intrinsic non-RRKM dynamics and non-random excitation is decomposition of the Cl^----CH_3Cl ion-dipole complex.[30] There is very slow IVR between the three intermolecular modes of the complex and the nine CH_3Cl intramolecular modes.[31] Thus, complexes formed by $Cl^- + CH_3Cl$ dissociate in accord with RRKM theory, but with only 3 active degrees of freedom and behaving like a small molecule.[32] The resulting classical unimolecular rate constant is in very good agreement with experiment.[33] Another example is the stereochemical unimolecular dynamics of trimethylene following different non-random initial excitations.[25,26] Classical trajectories and quantum dynamics give results in very good agreement.

In the work presented here comparison between classical and quantum unimolecular dynamics are extended by considering the decomposition of both classical and quantum[34] microcanonical ensembles. Classical trajectories are used to propagate the time evolution of each ensemble. In previous work,[35,36] quantum ensembles have been used to study the unimolecular decomposition of non-randomly excited molecules. The remainder of this article is organized as follows. Section II compares the classical and quantum RRKM theories for the decomposition of microcanonical ensembles. Section III describes the potential energy surfaces and chemical dynamics methodology used for the current calculations. The results are described in Sec. IV. The article ends with a discussion.

II. COMPARISON OF CLASSICAL AND QUANTUM RRKM THEORY

The RRKM unimolecular rate constant is derived using the concept of a transition state (TS) dividing surface in phase space and classical statistical mechanics,[17,37] and may be expressed as

$$k(E) = \frac{N^{\ddagger}(E - E_0)}{h\rho(E)}, \tag{4}$$

where $N^{\ddagger}(E)$ is the sum of states at the TS and ρ(E) is the density of states for the dissociating molecule. For completeness, the rate constant is also a function of angular momentum J, i.e., $k(E, J)$. However, to simplify the notation and, since only $J = 0$ is considered here, the rate constant is expressed as $k(E)$. The quantum RRKM rate constant results from replacing the classical $N^{\ddagger}(E)$ and $\rho(E)$ with their quantum counterparts.

As illustrated by Figure 1, classical and quantum RRKM theory have different representations of the reaction energetics. For the quantum RRKM calculation, E is the reactant energy above the zero-point level, i.e., E^R, and the TS's energy E-E_0 is $E^{\ddagger}$. For the classical RRKM calculation, E is the total energy $E_{total} = E^R + E^R_{ZP}$ and the TS's energy is $E^{\ddagger}_{total} = E^{\ddagger} + E^{\ddagger}_{ZP}$. For $E^R \gg E^R_{ZP}$ the quantum RRKM $k(E)$ approaches the classical RRKM $k(E)$. This may be illustrated by comparing the classical and quantum harmonic density of states $\rho(E)$. The classical $\rho_c(E)$ is $dN_c(E)/dE$ and given by[17]

$$\rho_c(E) = \frac{E^{s-1}}{\left[(s-1)! \prod_{i=1}^{s} h\nu_i\right]}, \tag{5}$$

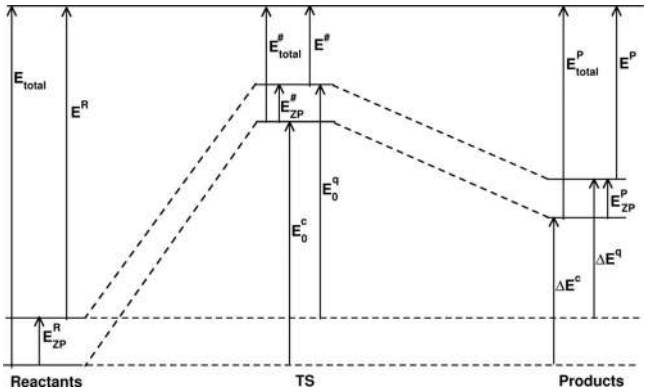

FIG. 1. Schematic representation of the energy level diagram showing the classical and quantum energies.

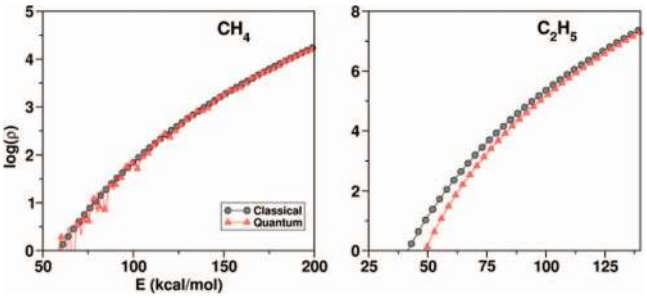

FIG. 2. Comparison of classical and quantum vibrational densities of state, ρ(E), for CH_4 and C_2H_5 versus energy.

where s is the number of vibrational modes and the ν_i their frequencies. The quantum $\rho_q(E)$ is found by enumerating the quantum number of states[38] at E and $E+\Delta E$, and forming the finite difference

$$\rho_q(E) = \frac{[N_q(E+\Delta E) - N_q(E)]}{\Delta E}. \quad (6)$$

The classical and quantum $\rho(E)$ are compared in Figure 2 for CH_4 and C_2H_5, two of the molecules considered here. The densities of states are plotted versus E_{total} and $\rho_q(E)$ is zero until E_{total} is greater than E^R_{ZP}. The quantum $\rho_q(E)$ approaches the classical $\rho_c(E)$ for large E_{total}. This concurs with the classical-quantum correspondence of statistical mechanics.[39] For high temperatures (i.e., energies), with respect to the spacings of the vibrational energy levels, the energy levels may be treated as continuous. Thus, at high temperatures the quantum harmonic oscillator partition function

$$Q_q = \prod_{i=1}^{s} \frac{1}{1 - e^{-h\nu_i/k_BT}} \quad (7)$$

becomes the classical partition function

$$Q_c = \prod_{i=1}^{s} \frac{k_BT}{h\nu_i} = \int_0^\infty \rho_c(E) e^{-E/k_BT} dE. \quad (8)$$

At high energies the quantum $\rho_q(E)$ and classical $\rho_c(E)$ becomes equivalent and the quantum density of states is given by the classical expression for $E_{total} = E^R + E^R_{ZP}$. Thus, the zero-point energy contributes to the density of states for the high energy limit. This is the "semi-classical" model of Marcus and Rice.[40] Rabinovitch and co-workers[41,42] amended this model so that a classical-like expression represents $\rho_q(E)$ for all energies. It is known as the Whitten-Rabinovitch semiempirical approximation[42] and given by

$$\rho_q(E) = \frac{\left(E^R + aE^R_{ZP}\right)^{s-1}}{(s-1)! \prod_{i=1}^{s} h\nu_i}, \quad (9)$$

where the factor a is a function of the reduced energy E^R/E^R_{ZP} and increases from zero at $E^R = 0$ to unity at high E^R to give the Marcus-Rice expression. The approach of the quantum RRKM $k(E)$ to the classical RRKM $k(E)$, at high energy, has been shown in previous work.[27]

III. POTENTIAL ENERGY SURFACES AND RRKM CALCULATIONS

In this work, unimolecular decomposition of the pre-reaction ion-dipole complex Cl^----CH_3Br in the familiar S_N2 reaction

$$Cl^- + CH_3Br \leftrightarrow Cl^- - - -CH_3Br$$
$$\leftrightarrow ClCH_3 - - -Br^- \rightarrow ClCH_3 + Br^-, \quad (10)$$

and the unimolecular decompositions of CH_4 and C_2H_5 are considered. Unimolecular decomposition of Cl^----CH_3Br is intrinsically non-RRKM,[43] while the CH_4 (Ref. 44) and C_2H_5 (Refs. 27 and 52) decompositions are intrinsically RRKM processes. Analytic potential energy functions were used to study Cl^----CH_3Br and CH_4 dissociation, while direct dynamics[45] was used to study C_2H_5 dissociation. The analytic potential energy surface (PES) for the Cl^----CH_3Br S_N2 reaction was developed by using *ab initio* calculations to modify[46] the analytic PES previously developed for the Cl^-+ CH_3Cl S_N2 reaction.[47] The analytic PES for CH_4 dissociation is the modified[44,48] Duchovic-Hase-Schlegel analytic potential energy function.[49]

The PES used for the $C_2H_5 \rightarrow H + C_2H_4$ direct dynamics calculations is the one given by UHF/4-31G theory. This is the electronic structure theory used to develop an analytic potential energy function for the C_2H_5 system,[50–52] which is used in chemical dynamics simulations.[27,53,54]

To compare with the chemical dynamics simulations, harmonic RRKM unimolecular rate constants were calculated[55] using the same PESs as used for the simulations. Variational transition states were found for $CH_4 \rightarrow H + CH_3$ and Cl^----$CH_3Br \rightarrow Cl^- + CH_3Br$ dissociation, since these dissociations do not have saddle points. Vibrational frequencies were found versus the intrinsic reaction co-ordinate[56,57] for each of these dissociations. These information was then used to find their vibrational variational TSs.[58] This model gives accurate TSs for the $CH_4 \leftrightarrow H + CH_3$ and Cl^----CH_3Br $\leftrightarrow Cl^- + CH_3Br$ reactive systems.[44,46]

The RRKM calculations for $C_2H_5 \rightarrow H + C_2H_4$ were performed as described previously.[59,60] The internal rotation barrier for C_2H_5 is quite low and this motion was treated as a free rotor with a symmetry number of 6. However, for the TS the internal rotation is a torsion, with a high barrier and a high frequency of 1185 cm^{-1}, and was treated as a vibration. It is of interest that there are no substantial changes in the RRKM rate constants if the C_2H_5 internal rotation is treated as a vibration with its 119 cm^{-1} frequency instead of as a free rotor. The ratio of the classical RRKM rate constants with the C_2H_5 internal rotation treated as a free rotor instead of as a vibrator is 1.03, 0.97, 0.92, 0.84, and 0.75 for the respective total energies considered here of 80, 90, 100, 120, and 150 kcal/mol.

IV. METHODOLOGY OF THE CHEMICAL DYNAMICS SIMULATIONS

The chemical dynamics simulations were performed with the computer program VENUS[61,62] and with VENUS coupled to the electronic structure theory software package

NWChem.[63,64] The analytic potential energy functions for Cl^----CH_3Br and CH_4 are in VENUS, and the UHF/4-31G PES used for the C_2H_5 direct dynamics was obtained from NWChem.

Fixed total energy, with $T_{rot} = 300$ K ($E_{rot} = 3RT/2$), initial conditions were chosen for the trajectories by sampling classical and quantum microcanonical ensembles,[34,36,65] using standard algorithms in VENUS. For the classical microcanonical sampling the classical phase space is sampled randomly, so that the $t = 0$ rate constant is the classical microcanonical (i.e., RRKM) rate constant. Quasiclassical sampling of the quantum microcanonical ensemble is performed for the same total energy E as for the classical microcanonical sampling, with the decomposing molecule's normal mode energy levels sampled randomly within the energy interval $E \rightarrow E + \Delta E$; with $\Delta E = 100$ cm^{-1}. Thus, the classical phase space at energy E is not sampled randomly for the quantum microcanonical ensemble.

For quasiclassical sampling of a microcanonical ensemble, a molecule consisting of s quantum harmonic oscillators has total energy

$$E = \sum_{i=1}^{s} E_i + E_{ZPE}, \tag{11}$$

where $E_i = n_i h\nu_i$ are the individual oscillator energies. A state $\mathbf{n}$ $(n_1, n_2, \ldots, n_s)$ is chosen at random in the energy interval $E \rightarrow E + \Delta E$. This is done by sampling the following relative probability oscillator j has energy E_j after energies have been randomly chosen for oscillators $1,2,\ldots,j-1$:

$$\frac{\rho_{s-j}\left(E - \sum_{i=1}^{j} E_i\right)}{\rho_{s-j}\left(E - \sum_{i=1}^{j-1} E_i\right)}. \tag{12}$$

Here ρ_{s-j} is the density of states for the remaining unsampled s-j oscillators. E_j is sampled randomly between zero and $E - \sum_{i=1}^{j-1} E_i$. The denominator is for the most probable value of E_j, which is zero. Complete details of the sampling algorithm are given in Ref. 34.

Ensembles of trajectories were calculated at different total energies E for both the classical and quantum microcanonical sampling. The trajectory ensembles were propagated to 25 ps, or until unimolecular dissociation occurred, using a 6th-order symplectic integrator.[66,67] The results are discussed in Sec. V.

V. RESULTS

A. Intrinsic RRKM dynamics

Previous chemical dynamics simulations have shown that the classical unimolecular dynamics of $C_2H_5 \rightarrow H + C_2H_4$ and $CH_4 \rightarrow H + CH_3$ dissociation are intrinsically RRKM.[27,44,53] In this section, the unimolecular decomposition of their classical and quantum microcanonical ensembles are compared.

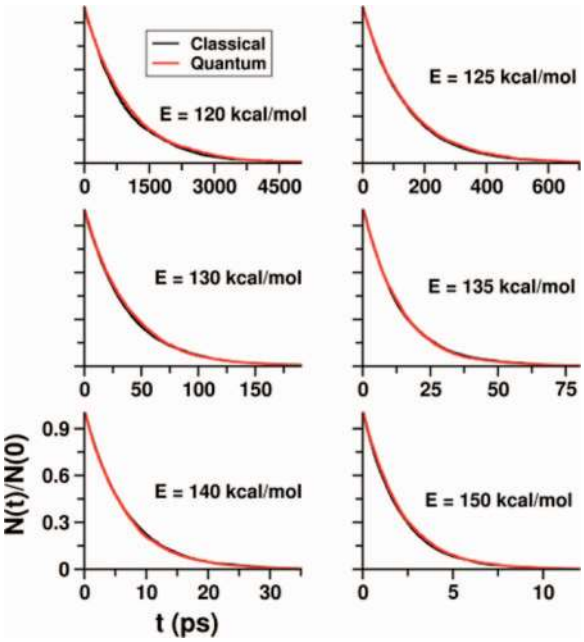

FIG. 3. Lifetime distributions $N(t)/N(0)$, for $CH_4 \rightarrow H + CH_3$ dissociation, resulting from classical trajectory simulations of initial classical and quantum microcanonical ensembles.

1. $CH_4 \rightarrow H + CH_3$ dissociation

The unimolecular dissociation of CH_4 was studied at energies E_{total} of 120, 125, 130, 135, 140, and 150 kcal/mol. $E_{ZP}^R = 29.2$ kcal/mol and the classical $CH_4 \rightarrow H + CH_3$ bond dissociation energy is 109.46 kcal/mol, for the analytic potential used for the simulations.[48,49] Plots of $N(t)/N(0)$ versus t are given in Figure 3 for the classical and quantum microcanonical ensembles. The plots for the classical ensembles are exponential with rate constant $k(E)$ and this rate constant is in excellent agreement with that for the initial classical microcanonical ensemble; i.e., $P(0)$ in Eq. (2). Thus, as found previously,[44] the classical dissociation of CH_4 is intrinsically RRKM.

As shown in Figure 3 plots of the $N(t)/N(0)$ distributions for the quantum microcanonical ensemble are also exponential and in excellent agreement with the distributions for the classical microcanonical ensemble. The rate constants $k(E)$ for the classical and quantum distributions are compared in Table I. They are very similar, with a largest difference for a 6% smaller quantum rate constant for the lowest E_{total} of 120 kcal/mol. Since the quantum microcanonical ensemble excites methane's classical phase space non-randomly, the initial short-time decomposition for this ensemble was carefully studied to see if its rate constant might be different, e.g., smaller, than that for the overall exponential decomposition. However, this was found not to be the case and the initial decomposition rate was the same as that for longer times. Apparently, the initial non-random classical phase space distribution for the quantum microcanonical ensemble is rapidly converted to a random classical phase space distribution by efficient IVR.

The trajectory rate constants, for the classical and quantum microcanonical ensembles, are compared with

TABLE I. Comparison of trajectory and harmonic RRKM classical and quantum rate constants for $CH_4 \rightarrow H + CH_3$ dissociation.[a]

	Trajectory[b]		Harmonic RRKM	
E_{total}[c]	k_c	k_q	k_c	k_q
120	1.06×10^{-3}	1.01×10^{-3}	2.66×10^{-3}	...[d]
125	7.16×10^{-3}	6.97×10^{-3}	2.33×10^{-2}	...
130	2.69×10^{-2}	2.61×10^{-2}	9.74×10^{-2}	...
135	7.09×10^{-2}	7.07×10^{-2}	2.92×10^{-1}	1.63×10^{-2}
140	1.49×10^{-1}	1.52×10^{-1}	6.74×10^{-1}	1.19×10^{-1}
150	4.89×10^{-1}	4.69×10^{-1}	2.34	7.26×10^{-1}

[a]The classical and quantum rate constants are k_c and k_q, respectively, and in unit of ps^{-1}.
[b]The trajectory rate constants are those for the exponential fits to the $N(t)/N(0)$ distributions, Figure 3, determined for the classical and quantum microcanonical ensembles.
[c]Energy is in unit of kcal/mol.
[d]The total energy is less than the energy needed for CH_4 to decompose with ZPE at the TS.

classical and quantum harmonic RRKM rate constants in Table I. For E_{total} of 130 kcal/mol and less, the total energy is less than the energy of the $H + CH_3$ products, including ZPE. Thus, the quantum RRKM rate constants are zero. At E_{total} = 135 kcal/mol the ratio of the classical and quantum harmonic RRKM rate constants is 18, while at the highest energy of 150 kcal/mol it is substantially smaller and 3. The classical harmonic RRKM rate constants are larger than those determined from the trajectory simulations. For the classical calculations the ratio of the trajectory and harmonic RRKM rate constants, i.e., $k_{traj}(E)/k_{RRKM}(E)$, is the anharmonic correction $f_{anh}(E)$ to the harmonic RRKM unimolecular rate constant.[68] The resulting values of $f_{anh}(E)$ are in the range of 0.39–0.21 and are similar to 0.42 found previously[44] for the similar PES at E = 127 kcal/mol. The previous study[44] used the stiff Morse function for the C–H stretch potential,[58,69] while the current work used the standard Morse function for this potential.

2. $C_2H_5 \rightarrow H + C_2H_4$ dissociation

The calculations for C_2H_5 dissociation were performed by direct dynamics at the UHF/4-31G level of theory. The distribution $N(t)/N(0)$ was determined for E_{total} in the range of 80–150 kcal/mol and the results are plotted in Figure 4. The classical dissociation energy is 43.5 kcal/mol and the quantum mechanical dissociation threshold, without tunneling, requires ZPE in the TS and is 78.2 kcal/mol.

As shown in Figure 4 the $N(t)/N(0)$ distribution is exponential for both the classical and quantum ensembles at the higher E_{total} energies of 120 and 150 kcal/mol. The $k(E)$ rate constants for the exponential fits are listed in Table II and there is good agreement between the values for the classical and quantum ensembles. For the lower E_{total} energies of 80–100 kcal/mol the classical $N(t)/N(0)$ remains exponential, but for the quantum ensemble this distribution becomes non-exponential and has an initial decay smaller than that for the classical ensemble. The non-exponential $N(t)/N(0)$ are fit by Eq. (3) with two exponentials and the fitting parameters are listed in Table III. The non-exponential characteristics of these $N(t)/N(0)$ are small. For the E_{total} of 80 and 90 kcal/mol the rate constants for the two exponentials are similar. For

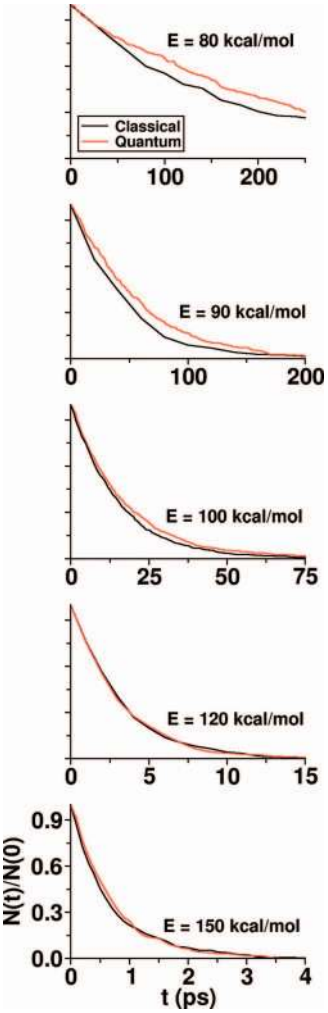

FIG. 4. Lifetime distributions $N(t)/N(0)$, for $C_2H_5 \rightarrow H + C_2H_4$ dissociation, resulting from classical trajectory simulations of initial classical and quantum microcanonical ensembles.

E_{total} = 100 kcal/mol, the exponential with the small rate constant makes only a 0.009 contribution to $N(t)/N(0)$.

The rate constants, for the initial classical and quantum microcanonical ensembles, are listed in Table II for E_{total} = 80–100 kcal/mol. The rate constant for the classical

TABLE II. Comparison of trajectory and harmonic RRKM classical and quantum rate constants for $C_2H_5 \rightarrow H + C_2H_4$ dissociation.[a]

	Trajectory[b]		Harmonic RRKM	
E_{total}[c]	k_c	k_q	k_c	k_q
80	5.33×10^{-3}	4.87×10^{-3}	3.33×10^{-3}	3.82×10^{-5}
90	2.23×10^{-2}	1.76×10^{-2}	2.16×10^{-2}	4.68×10^{-3}
100	6.59×10^{-2}	5.89×10^{-2}	8.28×10^{-2}	3.98×10^{-2}
120	3.18×10^{-1}	3.19×10^{-1}	5.13×10^{-1}	4.33×10^{-1}
150	1.49	1.41	2.66	2.88

[a]The classical and quantum rate constants are k_c and k_q, respectively, and in unit of ps^{-1}.
[b]The k_q trajectory rate constants for E_{total} of 120 and 150 kcal/mol and the k_c trajectory rate constants are those for the exponential fits to the $N(t)/N(0)$ distributions, Figure 4, determined for the quantum and classical microcanonical ensembles. The trajectory k_q rate constants for E_{total} of 80–100 kcal/mol were determined from the non-exponential fits to $N(t)/N(0)$, Eqs. (3) and (13).
[c]Energy is in unit of kcal/mol.

TABLE III. Eq. (3) fitting parameters for the non-exponential $N(t)/N(0)$.[a]

E_{total}	f_1	f_2	f_3	k_1	k_2	k_3
C_2H_5, Quantum microcanonical						
80	0.890	0.110	...	0.005	0.003	...
90	0.090	0.910	...	0.019	0.017	...
100	0.990	0.009	...	0.059	0.011	...
Cl^----CH_3Br, Classical microcanonical						
30	0.229	0.379	0.391	0.426	0.045	0.021
35	0.236	0.231	0.533	0.804	0.182	0.044
40	0.389	0.238	0.373	0.817	0.174	0.062
45	0.306	0.318	0.376	1.335	0.381	0.095
50	0.059	0.529	0.411	20.87	0.915	0.144
60	0.108	0.599	0.293	20.51	1.042	0.216
Cl^----CH_3Br, Quantum microcanonical						
30	0.019	0.166	0.815	0.458	0.081	0.025
35	0.122	0.327	0.551	0.518	0.094	0.038
40	0.242	0.434	0.325	0.758	0.109	0.058
45	0.266	0.215	0.519	1.082	0.402	0.103
50	0.057	0.437	0.506	17.72	0.873	0.149
60	0.090	0.639	0.270	21.55	0.931	0.196

[a]The sum of f_1, f_2, and f_3 is set to unity in the fitting, the k's are in unit of ps^{-1}, and E_{total} is in unit of kcal/mol.

ensemble is that for its exponential $N(t)/N(0)$. The rate constant for the non-exponential $N(t)/N(0)$, of the quantum microcanonical ensemble, is given by $P(0)$ of the lifetime distribution, Eq. (2), which is

$$k(E) = \sum_i f_i k_i. \tag{13}$$

For E_{total} of 80–100 kcal/mol the microcanonical rate constant for the quantum ensemble is smaller than that for the classical ensemble.

The trajectory rate constants for the classical and quantum microcanonical ensembles are compared with the harmonic RRKM values in Table II for the E_{total} of 80–150 kcal/mol. The ratio of the classical and quantum trajectory rate constants, i.e., $k_c(E)/k_q(E)$, is small and ranges from 1.00 to 1.27. It is similar for the low and high energies. For the classical and quantum RRKM rate constants this ratio decreases substantially from 87 to 0.92 as the energy is increased from 80 to 150 kcal/mol. The ratio $f_{anh}(E) = k_{traj}(E)/k_{RRKM}(E)$ for the classical calculations decreases from 1.62 to 0.56 as the energy is increased from 80 to 150 kcal/mol. A value for the anharmonic correction larger than unity is interesting and unusual.[17] For the quantum microcanonical ensemble it is uncertain whether $k_{traj}(E)/k_{RRKM}(E)$ identifies an anharmonic correction (see Sec. VI). Nevertheless, this ratio varies from 127 to 0.49 as the energy is increased.

In previous work the classical anharmonic microcanonical rate constant, for $C_2H_5 \rightarrow H + C_2H_4$ dissociation at 100 kcal/mol, was determined from a trajectory simulation[27] based on an analytic PES fit to UHF/4-31G calculations.[51] This rate constant is 1.4×10^{11} s^{-1} in comparison to the classical harmonic RRKM value of 7.3×10^{11} s^{-1},[70] which corresponds to an anharmonic correction factor f_{anh} of 0.2. In comparison, for the current study at 100 kcal/mol f_{anh} is 0.8 as shown in Table II. Thus, this analytic PES has substantially more anharmonicity than does the actual UHF/4-31G PES. In addition, the TS for the analytic PES is substantially "looser" than that for the UHF/4-31G PES, giving rise to a harmonic RRKM rate constant approximately ten times larger for the former.

TABLE IV. Comparison of trajectory and harmonic RRKM classical and quantum rate constants for the unimolecular decomposition of Cl^----CH_3Br.[a]

	Trajectory[b]		Harmonic RRKM[c]	
E_{total}[d]	k_c	k_q	k_c	k_q
30	1.23×10^{-1}	4.30×10^{-2}	7.28×10^{-1}	...[e]
35	2.55×10^{-1}	1.15×10^{-1}	1.26	1.19×10^{-1}
40	3.82×10^{-1}	2.49×10^{-1}	1.52	5.92×10^{-1}
45	5.65×10^{-1}	4.28×10^{-1}	1.72	1.18
50	1.79	1.47	1.89	1.44
60	2.89	2.59	2.16	1.81

[a]The classical and quantum rate constants are k_c and k_q, respectively, and in unit of ps^{-1}.
[b]The trajectory RRKM rate constants are found by Eq. (13).
[c]Harmonic RRKM rate constants are the sum of rate constants for the two paths, viz., Cl^----CH_3Br decomposition to Cl^- + CH_3Br and isomerization to $ClCH_3$---Br^-.
[d]Energy is in unit of kcal/mol.
[e]The total energy is less than the energy needed for Cl^----CH_3Br to decompose with ZPE at the TS.

B. Intrinsic non-RRKM dynamics

The calculations for Cl^----CH_3Br were performed using an analytic PES[46] and for E_{total} of 30–60 kcal/mol. This species may dissociate to Cl^- + CH_3Br or isomerize to $ClCH_3$---Br^- with classical thresholds of 10.74 and 7.83 kcal/mol, respectively. Including ZPE for the CH_3Br product and the $[Cl$--CH_3--$Br]^-$ central barrier, the quantum E_{total} respective thresholds are 34.44 and 31.73 kcal/mol.

Previous simulations and experiments have shown that the decomposition of Cl^----CH_3Br is expected to be intrinsically non-RRKM with non-exponential $N(t)/N(0)$ distributions.[30–33,43,71,72] As shown in Figure 5, this is indeed the finding for both the classical and quantum initial microcanonical ensembles. At the lower energies the initial decay of $N(t)/N(0)$ is slower for the quantum ensemble, while at the highest energy the decay of the classical and quantum ensembles are similar. The fits to the $N(t)/N(0)$, shown in Figure 5, were made with a sum of three exponentials and the fitting parameters for Eq. (3) are listed in Table III. The variation in the k_i rate constants for a particular fit is as large as two orders of magnitude. The initial rate constants for the classical and quantum microcanonical ensembles are the microcanonical values given by Eq. (13) and are listed in Table IV. For the lower E_{total}, the rate constant for the quantum ensemble is substantially smaller than that for the classical ensemble, while for the higher E_{total} the rate constants for the two ensembles are similar; i.e., findings consistent with the $N(t)/N(0)$ for the classical and quantum ensembles.

The harmonic RRKM rate constants for Cl^----CH_3Br decomposition are listed in Table IV, where they are compared with the trajectory rate constants. Cl^----CH_3Br decomposes to both Cl^- + CH_3Br and $ClCH_3$---Br^- and the RRKM rate

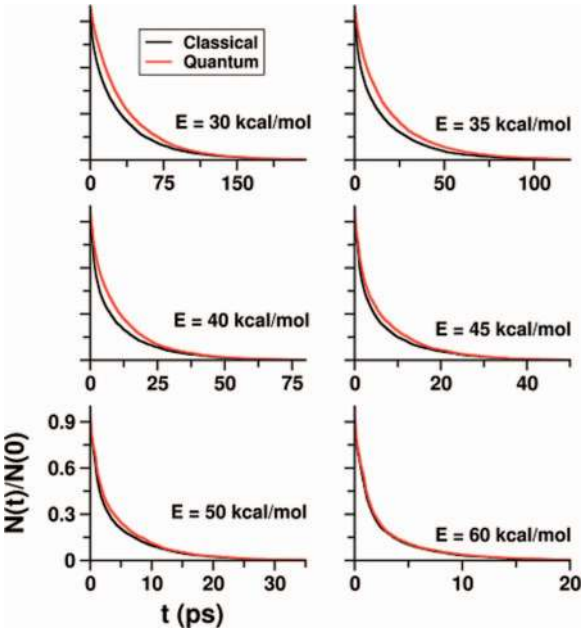

FIG. 5. Lifetime distributions $N(t)/N(0)$, for the unimolecular decomposition of Cl^----CH_3Br, resulting from classical trajectory simulations of initial classical and quantum microcanonical ensembles.

constants are the sum of the rate constants for these two paths. For the lower energies both the classical and quantum RRKM rate constants are larger than the respective trajectory rate constants for the classical and quantum microcanonical ensembles. However, for the highest energy of 60 kcal/mol the trajectory rate constants are larger. The ratio $k_{traj}(E)/k_{RRKM}(E)$ for the classical calculation ranges from 0.17 to 1.34 and gives the anharmonic correction f_{anh}(E) to classical harmonic RRKM rate constant. For the quantum calculations this ratio varies from 0.36 to 1.43.

The anharmonic correction $f_{anh}(E)$ to the RRKM rate constant is related to the ratios of anharmonic (*anh*) and harmonic (*h*) TS sums of states and reactant densities of state and is given by $N^{\neq}_{anh}(E\text{-}E_0)/N^{\neq}_{h}(E\text{-}E_0)$ divided by $\rho_{anh}(E)/\rho_h(E)$.[68] For E near the threshold the anharmonic correction for the TS sum of states is expected to be small,[17,68] so that $f_{anh}(E)$ is approximated by $\rho_h(E)/\rho_{anh}(E)$. The lower energy, 30–40 kcal/mol, values of 0.17–0.25 for the classical f_{anh}(E) may approximate $\rho_h(E)/\rho_{anh}$(E). These values for $f_{anh}(E)$ are similar to the classical $\rho_h(E)/\rho_{anh}$(E) ratios of ~0.5 found previously[30] for the Cl^----CH_3Cl complex for energies of 35–37 kcal/mol, assuming the CH_3Cl vibrational modes are harmonic oscillators. Including anharmonicity in these modes is expected to lower the f_{anh}(E) and make it closer to the current trajectory values. As the energy is increased the $N^{\neq}_{anh}(E\text{-}E_o)/N^{\neq}_{h}(E\text{-}E_0)$ term is expected to exceed unity and become important. The values of ~1.0 and larger for the Cl^----CH_3Br $f_{anh}(E)$, at the higher energies, are consistent with this expectation.

For the RRKM calculations, the quantum rate constant is smaller than the classical rate constant, a relationship that is mirrored by the trajectory calculations for the quantum and classical microcanonical ensembles. The E_{total} of 30 kcal/mol is less than the energies of 34.44 and 31.73 kcal/mol for the quantum harmonic thresholds to form Cl^- + CH_3Br and CH_3Cl + Br^-, and it is of interest that the trajectory rate constant for the quantum microcanonical ensemble is not zero in contrast to the harmonic RRKM rate constant. The anharmonic thresholds will be lower than the above values, and the anharmonic threshold for forming CH_3Cl + Br^- may be less than 30 kcal/mol. However, both Cl^- + CH_3Br and CH_3Cl + Br^- were formed in the 30 kcal/mol simulations, and the anharmonic threshold for forming Cl^- + CH_3Br is expected to exceed this energy.

For E_{total} of 35 kcal/mol the ratio of the classical and quantum rate constants, k_c/k_q, is 2.22 and 10.6 from the trajectory and harmonic RRKM calculations, respectively. Using anharmonic thresholds in the RRKM calculation will lower the RRKM ratio and make it closer to the trajectory ratio. For the E_{total} of 40–60 kcal/mol, the trajectory and harmonic RRKM k_c/k_q ratios are in overall good agreement.

VI. DISCUSSION

Previous studies, for Cl^- + $CH_3Cl \leftrightarrow Cl^-$---$CH_3Cl$,[30–33,72] trimethylene isomerization,[25,26] and relaxation of the C–H stretch overtone state in benzene,[14–16] have shown that classical dynamics often gives accurate short-time unimolecular and intramolecular dynamics for randomly prepared molecular states. The question addressed here is if classical chemical dynamics gives an accurate quantum microcanonical unimolecular rate constant for an initial quantum microcanonical ensemble of states. Quasiclassical sampling is performed for the quantum microcanonical ensemble. The unimolecular reactions considered are $CH_4 \rightarrow H + CH_3$, $C_2H_5 \rightarrow H + C_2H_4$, and decomposition of the ion-dipole complex Cl^----CH_3Br to Cl^- + CH_3Br and $ClCH_3$---Br^-.

In contrast to a classical microcanonical ensemble, the phase space is not sampled randomly by a quantum microcanonical ensemble. For the latter, there is ZPE in each degree of freedom and states are populated randomly in the energy interval $E \rightarrow \Delta E$, instead of sampling points at random on a constant energy shell as is done for the classical microcanonical ensemble. As a result of these differences, the classical microcanonical rate constant is larger than the quantum microcanonical rate constant. This may be understood by considering the classical expression for the unimolecular rate constant as an average flux moving past the TS towards products,[73] i.e.,

$$k(E) = \frac{\int \dots \int \dot{q}_1 dq_1 \dots dq_{3n} dp_1 \dots dp_{3n} \delta(q_1 - q_1^{\ddagger}) \delta(E - H)}{\int \dots \int dq_1 \dots dq_{3n} dp_1 \dots dp_{3n} \delta(E - H)}. \quad (14)$$

Without the constraint of having ZPE in the modes orthogonal to the reaction coordinate, the average value of the reaction coordinate velocity (momentum) will be larger for the classical microcanonical ensemble than for the quantum microcanonical ensemble.

A classical simulation of an initial microcanonical ensemble of states is expected to give an accurate quantum mechanical microcanonical rate constant if tunneling is unimportant and if the initial classical dynamics is vibrationally adiabatic. With the latter, the trajectories will retain ZPE in the modes orthogonal to the reaction coordinate motion as the trajectories cross the TS to form products. This is the nature of the dynamics Heller[74,75] had in mind for his frozen gaussians, i.e., short-time vibrationally adiabatic dynamics. The vibrationally adiabatic dynamics is not only required for the TS,[76] but also for the excited molecule as it approaches the TS. However, if instead there is extensive coupling between the vibrational modes, leading to rapid IVR and chaotic dynamics, ZPEs will not be conserved in accessing the TS and the classical chemical dynamics rate constant for the initial quantum microcanonical ensemble is expected to be the classical microcanonical rate constant.

Different unimolecular dynamics are found for the classical trajectory simulations of the initial quantum microcanonical ensembles for CH_4, C_2H_5 and Cl^----CH_3Br. For CH_4 dissociation, the classical simulation of the quantum microcanonical ensemble gives a rate constant identical to that found for the classical microcanonical ensemble. The quantum microcanonical ensemble decays in accord with ergodic dynamics and the prediction of classical RRKM theory. The results for C_2H_5 dissociation are mixed. As shown in Figure 4, for the lower energies of 80, 90, and 100 kcal/mol the classical simulation of the quantum microcanonical ensemble gives a rate constant smaller than that obtained from the classical microcanonical ensemble, the result expected by RRKM theory. However, as given in Table II, the initial rate constant for the quantum microcanonical ensemble is decidedly greater than that of quantum harmonic RRKM theory. It is doubtful that these differences can be explained by anharmonic effects. Thus, at these lower energies the classical simulation of the quantum microcanonical ensemble recovers some but not all of the dynamics predicted by quantum RRKM theory. For the higher energies of 120 and 150 kcal/mol, the classical simulations of the quantum microcanonical ensembles give unimolecular dynamics in accord with the ergodic and RRKM dynamics found for the classical microcanonical ensembles.

For the above two chemical systems, the classical dynamics is ergodic and in accord with the predictions of classical RRKM theory. In contrast, for Cl^----CH_3Br decomposition the classical unimolecular dynamics is intrinsically non-RRKM (Figure 5) and the classical simulation of a quantum microcanonical ensemble for Cl^----CH_3Br decomposition gives a rate constant which mimics the prediction of RRKM theory (Table IV). At E_{total} = 35 kcal/mol the trajectory rate constant for the quantum mechanical ensemble is approximately a factor of two too large as expected from an anharmonic correction (i.e., $k_q(harmonic)/k_q(anharmonic)$ is expected to be ~0.5 for the lower energies).[30] However, this correction does not include an anharmonic correction to the ZPE barriers for Cl^----CH_3Br decomposition, and this correction will increase the harmonic RRKM rate constant and possibly bring it into agreement with the trajectory quantum value. The lowest E_{total} of 30 kcal/mol is expected to be less than the anharmonic barrier for Cl^----CH_3Br decomposition to $Cl^- + CH_3Br$. Thus, this decomposition pathway observed in the classical simulation of the quantum microcanonical ensemble for this energy is in apparent disagreement with quantum RRKM theory. However, for the remaining energies of 35–60 kcal/mol, the classical simulations of the quantum microcanonical ensembles give rate constants in good agreement with the quantum RRKM values.

It should be noted that, though classical simulations of the quantum microcanonical ensembles for CH_4 and C_2H_5 do not give rate constants in agreement with quantum RRKM theory and presumably experiment, it is possible that classical simulations may give accurate short-time IVR and unimolecular rates for highly non-random initial states for these molecules. This is a topic of interest for future investigations.

In contrast to the intrinsic RRKM dynamics found here for C_2H_5 dissociation using UHF/4-31G direct dynamics, other direct dynamics simulations of the intramolecular and unimolecular dynamics of C_2H_5 (Refs. 77 and 78) suggest that a fraction of the C_2H_5 phase space consists of vague tori[20] and quasiperiodic[28] trajectories. The extent of this non-RRKM behavior depends on the level of electronic structure used for the direct dynamics.[77] A 5 eV excitation energy was investigated and it was found that ~78% of a microcanonical ensemble of trajectories dissociates to $H + C_2H_4$ with a single exponential and a rate constant consistent with RRKM theory.[77] However, the remaining long-lived trajectories have motions consistent with vague tori and quasiperiodicity and a low degree of ergodicity.[78] These dynamics indicate that C_2H_5 dissociation is intrinsically non-RRKM at high energies. It is suggested[77] that these long-lived trajectories are prepared when C_2H_5 is photoexcited[79,80] and explain observed dissociation lifetimes which are several orders of magnitude longer than those expected from RRKM theory. Such trajectories are not present in the UHF/4-31G direct dynamics reported here. The possible sensitivity of intramolecular dynamics, and intrinsic RRKM and non-RRKM behavior, on the electronic structure theory method used for the direct dynamics simulation is quite intriguing. It is an important topic for future intramolecular and unimolecular studies of C_2H_5 and other molecules.

Finally, for future work it is of interest to sample the normal mode momenta **P** and coordinates **Q**, for the quantum microcanonical ensemble, in accord with their quantum distributions.[81] This sampling may be performed at a constant energy, as recently described for sampling the Wigner distribution for a molecule's ZPE level.[82] For the quasiclassical sampling performed here, for state **n**, a fixed number of quanta n_i are added to the i-th normal mode and the classical phase's for the modes are chosen randomly. By sampling the **P** and **Q** quantum distributions for a specific state **n** of the molecule, there will not be a fixed n_i for the i-th mode and, instead, the average energy in the mode will equal that for level n_i.[82] It would also be of interest to sample the Husimi distribution[83] for the quantum microcanonical ensemble.

ACKNOWLEDGMENTS

This material is based upon work supported by the National Science Foundation under Grant No. CHE-0957521 and the Robert A. Welch Foundation under Grant No. D-0005. Support was also provided by the High Performance Computing Center (HPCC) at Texas Tech University, under the direction of Philip W. Smith.

[1]D. L. Bunker, J. Chem. Phys. **37**, 393 (1962).
[2]D. L. Bunker, J. Chem. Phys. **40**, 1946 (1964).
[3]D. L. Bunker and W. L. Hase, J. Chem. Phys. **59**, 4621 (1973).
[4]J. S. Hutchinson, W. P. Reinhardt, and J. T. Hynes, J. Chem. Phys. **79**, 4247 (1983).
[5]K. N. Swamy and W. L. Hase, J. Chem. Phys. **82**, 123 (1985).
[6]B. K. Carpenter, Annu. Rev. Phys. Chem. **56**, 57 (2005).
[7]G. S. Ezra, H. Waalkens, and S. Wiggins, J. Chem. Phys. **130**, 164118 (2009).
[8]U. Lourderaj and W. L. Hase, J. Phys. Chem. A **113**, 2236 (2009).
[9]C. C. Martens, M. J. Davis, and G. S. Ezra, Chem. Phys. Lett. **142**, 519 (1987).
[10]D. W. Oxtoby and S. A. Rice, J. Chem. Phys. **65**, 1676 (1976).
[11]R. J. Wolf and W. L. Hase, J. Chem. Phys. **72**, 316 (1980).
[12]D.-H. Lu, W. L. Hase, and R. J. Wolf, J. Chem. Phys. **85**, 4422 (1986).
[13]A. García-Ayllón, J. Santamaria, and G. S. Ezra, J. Chem. Phys. **89**, 801 (1988).
[14]E. L. Sibert, III, J. T. Hynes, and W. P. Reinhardt, J. Chem. Phys. **81**, 1135 (1984).
[15]D.-H. Lu and W. L. Hase, J. Phys. Chem. **92**, 3217 (1988).
[16]R. E. Wyatt, C. Iung, and C. Leforestier, J. Chem. Phys. **97**, 3477 (1992).
[17]T. Baer and W. L. Hase, *Unimolecular Reaction Dynamics. Theory and Experiments* (Oxford University Press, New York, 1996).
[18]O. K. Rice, Z. Phys. Chem. **7**, 226 (1930).
[19]W. L. Hase, R. J. Duchovic, K. N. Swamy, and R. J. Wolf, J. Chem. Phys. **80**, 714 (1984).
[20]R. B. Shirts and W. P. Reinhardt, J. Chem. Phys. **77**, 5204 (1982).
[21]R. E. Gillilan and G. S. Ezra, J. Chem. Phys. **94**, 2648 (1991).
[22]S. Yu. Grebenshchikov, R. Schinke, and W. L. Hase, *Unimolecular Kinetics Part I. The Reaction Step*, Comprehensive Chemical Kinetics, Vol. 39, edited by N. J. B. Green (Elsevier, New York, 2003), p. 105.
[23]A. J. Dobbyn, M. Stumpf, H.-M. Keller, and R. Schinke, J. Chem. Phys. **104**, 8357 (1996).
[24]S. Yu. Grebenshchikov, C. Beck, H. Flöthman, R. Schinke, and S. Kato, J. Chem. Phys. **111**, 619 (1999).
[25]C. Doubleday, Jr., K. Bolton, G. H. Peslherbe, and W. L. Hase, J. Am. Chem. Soc. **118**, 9922 (1996).
[26]E. M. Goldfield, Faraday Discuss. **110**, 185 (1998).
[27]W. L. Hase and D. G. Buckowski, J. Comput. Chem. **3**, 335 (1982).
[28]W. L. Hase, J. Phys. Chem. **86**, 2873 (1982).
[29]E. J. Heller, J. Phys. Chem. A **103**, 10433 (1999).
[30]G. H. Peslherbe, H. Wang, and W. L. Hase, J. Chem. Phys. **102**, 5626 (1995).
[31]S. R. Vande Linde and W. L. Hase, J. Chem. Phys. **93**, 7962 (1990).
[32]S. R. Vande Linde and W. L. Hase, J. Phys. Chem. **94**, 6148 (1990).
[33]J. Mikosch, R. Otto, S. Trippel, C. Eichhorn, M. Weidemüller, and R. Wester, J. Phys. Chem. A **112**, 10448 (2008).
[34]K. Park, J. Engelkemier, M. Persico, P. Manikandan, and W. L. Hase, J. Phys. Chem. A **115**, 6603 (2011).
[35]C. S. Sloane and W. L. Hase, J. Chem. Phys. **66**, 1523 (1977).
[36]G. H. Peslherbe, H. Wang, and W. L. Hase, Adv. Chem. Phys. **105**, 171 (1999).
[37]W. Forst, *Theory of Unimolecular Reactions* (Academic, New York, 1973).
[38]T. Beyer and D. R. Swinehart, ACM Commun. **16**, 379 (1973).
[39]D. A. McQuarrie, *Statistical Mechanics* (Harper, New York, 1976).
[40]R. A. Marcus and O. K. Rice, J. Phys. Colloid Chem. **55**, 894 (1951).
[41]B. S. Rabinovitch and R. W. Diesen, J. Chem. Phys. **30**, 735 (1959).
[42]G. Z. Whitten and B. S. Rabinovitch, J. Chem. Phys. **38**, 2466 (1963).
[43]H. Wang, G. H. Peslherbe, and W. L. Hase, J. Am. Chem. Soc. **116**, 9644 (1994).
[44]X. Hu and W. L. Hase, J. Chem. Phys. **95**, 8073 (1991).
[45]L. Sun and W. L. Hase, Rev. Comput. Chem. **19**, 79 (2003).
[46]H. Wang, L. Zhu, and W. L. Hase, J. Phys. Chem. **98**, 1608 (1994).
[47]S. R. Vande Linde and W. L. Hase, J. Phys. Chem. **94**, 2778 (1990).
[48]W. L. Hase, S. L. Mondro, R. J. Duchovic, and D. M. Hirst, J. Am. Chem. Soc. **109**, 2916 (1987).
[49]R. J. Duchovic, W. L. Hase, and H. B. Schlegel, J. Phys. Chem. **88**, 1339 (1984).
[50]C. S. Sloane and W. L. Hase, Faraday Discuss. Chem. Soc. **62**, 210 (1977).
[51]W. L. Hase, G. Mrowka, R. J. Brudzynski, and C. S. Sloane, J. Chem. Phys. **69**, 3548 (1978); erratum: J. Chem. Phys. **72**, 6321 (1980).
[52]W. L. Hase, R. J. Wolf, and C. S. Sloane, J. Chem. Phys. **71**, 2911 (1979); erratum: J. Chem. Phys. **76**, 2771 (1982).
[53]W. L. Hase, D. G. Buckowski, and K. N. Swamy, J. Phys. Chem. **87**, 2754 (1983).
[54]W. L. Hase, D. M. Ludlow, R. J. Wolf, and T. Schlick, J. Phys. Chem. **85**, 958 (1981).
[55]L. Zhu and W. L. Hase, Quant. Chem. Prog. Exch. Bull. **14**, 644 (1994).
[56]K. Fukui, J. Phys. Chem. **74**, 4161 (1970).
[57]W. H. Miller, N. C. Handy, and J. E. Adams, J. Chem. Phys. **72**, 99 (1980).
[58]W. L. Hase and R. J. Duchovic, J. Chem. Phys. **83**, 3448 (1985).
[59]W. L. Hase and H. B. Schlegel, J. Phys. Chem. **86**, 3901 (1982).
[60]W. L. Hase, H. B. Schlegel, V. Balbyshev, and M. Page, J. Phys. Chem. **100**, 5354 (1996).
[61]W. L. Hase, R. J. Duchovic, X. Hu, A. Komornicki, K. F. Lim, D.-H. Lu, G. H. Peslherbe, K. N. Swamy, S. R. Vande Linde, A. Varandas, H. Wang, and R. J. Wolf, Quant. Chem. Prog. Exch. Bull. **16**, 671 (1996).
[62]X. Hu, W. L. Hase, and T. Pirraglia, J. Comput. Chem. **12**, 1014 (1992).
[63]E. J. Bylaska, W. A. de Jong, N. Govind, K. Kowalski, T. P. Straatsma, M. Valiev, D. Wang, E. Apra, T. L. Windus, J. Hammond, P. Nichols, S. Hirata, M. T. Hackler, Y. Zhao, P.-D. Fan, R. J. Harrison, M. Dupuis, D. M. A. Smith, J. Nieplocha, V. Tipparaju, M. Krishnan, A. Vazquez-Mayagoitia, Q. Wu, T. Van Voorhis, A. A. Auer, M. Nooijen, L. D. Crosby, E. Brown, G. Cisneros, G. I. Fann, H. Fruchtl, J. Garza, K. Hirao, R. Kendall, J. A. Nichols, K. Tsemekhman, K. Wolinski, J. Anchell, D. Bernholdt, P. Borowski, T. Clark, D. Clerc, H. Dachsel, M. Deegan, K. Dyall, D. Elwood, E. Glendening, M. Gutowski, A. Hess, J. Jaffe, B. Johnson, J. Ju, R. Kobayashi, R. Kutteh, Z. Lin, R. Littlefield, X. Long, B. Meng, T. Nakajima, S. Niu, L. Pollack, M. Rosing, G. Sandrone, M. Stave, H. Taylor, G. Thomas, J. van Lenthe, A. Wong, and Z. Zhang, *NWchem, A Computational Chemistry Package for Parallel Computers, Version 5.1.1* (Pacific Northwest National Laboratory, Richland, Washington, 2009).
[64]M. Valiev, E. J. Bylaska, N. Govind, K. Kowalski, T. P. Straatsma, H. J. J. van Dam, D. Wang, J. Nieplocha, E. Apra, T. L. Windus, and W. A. de Jong, Comput. Phys. Commun. **181**, 1477 (2010).
[65]W. L. Hase and D. G. Buckowski, Chem. Phys. Lett. **74**, 284 (1980).
[66]C. Schlier and A. Seiter, J. Phys. Chem. A **102**, 9399 (1998).
[67]C. Schlier and A. Seiter, Comput. Phys. Commun. **130**, 176 (2000).
[68]K. Song and W. L. Hase, J. Chem. Phys. **110**, 6198 (1999).
[69]R. J. Duchovic and W. L. Hase, Chem. Phys. Lett. **110**, 6198 (1984).
[70]The analytic PES (Ref. 51) only allows one of the H-atoms to dissociate and the actual trajectory rate constant is 4.5×10^{10} s^{-1} (Ref. 27). This rate constant is multiplied by three to increase the reaction path degeneracy from one to three.
[71]D. S. Tonner and T. B. McMahon, J. Am. Chem. Soc. **122**, 8783 (2000).
[72]R. Wester, A. E. Bragg, A. V. Davis, and D. M. Neumark, J. Chem. Phys. **119**, 10032 (2003).
[73]J. D. Doll, J. Chem. Phys. **73**, 2760 (1980).
[74]E. J. Heller, J. Chem. Phys. **62**, 1544 (1975).
[75]E. J. Heller, J. Chem. Phys. **75**, 2923 (1981).
[76]J. C. Lorquet, J. Phys. Chem. A **115**, 4610 (2011).
[77]A. Bach, J. M. Hostettler, and P. Chen, J. Chem. Phys. **123**, 021101 (2005).
[78]A. Bach, J. M. Hostettler, and P. Chen, J. Chem. Phys. **125**, 024304 (2006).
[79]T. Gilbert, T. L. Grebner, I. Fischer, and P. Chen, J. Chem. Phys. **110**, 5485 (1999).
[80]G. Amaral, K. S. Xu, and J. S. Zhang, J. Chem. Phys. **114**, 5164 (2001).
[81]G. Granucci and M. Persico, private communication (2011).
[82]L. Sun and W. L. Hase, J. Chem. Phys. **133**, 044313 (2010).
[83]K. Husimi, Proc. Phys. Math. Soc. Jpn. **22**, 264 (1940).